

Low lncRNA ZNF385D-AS2 expression and its prognostic significance in liver cancer

ZE ZHANG¹, SHOUQIAN WANG¹, YAHUI LIU¹, ZIHUI MENG² and FANGFANG CHEN³

¹Department of General Surgery, The First Hospital of Jilin University, Changchun, Jilin 130021; Departments of ²Hepatobiliary-Pancreatic Surgery, ³Gastrointestinal Colorectal and Anal Surgery, China-Japan Union Hospital of Jilin University, Changchun, Jilin 130033, P.R. China

Received April 3, 2019; Accepted July 10, 2019

DOI: 10.3892/or.2019.7238

Abstract. Hepatocellular carcinoma (HCC) is a common digestive system disease with no curative treatment. Zinc finger protein 385D antisense RNA 2 (ZNF385D-AS2) is a long non-coding RNA (lncRNA) that has been predicted to function in human diseases, including several types of cancer. Yet, it has not been investigated in relation to liver cancer. Thus, the present study was designed with an aim to elucidate the prognostic significance of lncRNA ZNF385D-AS2 in HCC. The Cancer Genome Atlas-Liver Hepatocellular Carcinoma (TCGA-LIHC) collection of data was utilized to analyze the expression of lncRNA ZNF385D-AS2 in liver cancer. Then Chi-square tests were used to evaluate the correlation between clinical characteristics and lncRNA ZNF385D-AS2 expression. The significance of lncRNA ZNF385D-AS2 in patient prognosis was evaluated using Kaplan-Meier curves and Cox analysis. Concomitantly, Gene Set Enrichment Analysis (GSEA) was performed to analyze the most closely related cytological behavior. Finally, we used the Database for Annotation, Visualization and Integrated Discovery (DAVID) and KOBAS software and data from the Gene Expression Omnibus (GEO) database to analyze the possible competing endogenous RNA (ceRNA) network pattern as well as the co-expression network in liver cancer. Based on the results, analysis of RNA-Seq gene expression data for 303 patients with primary tumors revealed low expression of ZNF385D-AS2 in liver cancer. Low expression of ZNF385D-AS2 was found to be significantly associated with sex ($P=0.050$), T stage ($P=0.049$), M stage ($P=0.040$),

N stage ($P<0.001$) and clinical stage ($P=0.037$). Patients with ZNF385D-AS2 low-expression liver cancers had a shorter median overall survival compared with the patients with ZNF385D-AS2 high-expression liver cancers ($P=0.0079$). Cox analysis identified ZNF385D-AS2 low-expression as an independent prognostic variable ($AUC=0.594$) for overall survival in liver cancer patients. Co-expression and ceRNA predictive analysis data suggested that there may be a regulatory signaling axis between ZNF385D-AS2 and miR-96 and miR-182. In conclusion, our results suggests that low expression of ZNF385D-AS2 is predictive of a poor prognosis of liver cancer patients.

Introduction

Hepatocellular carcinoma (HCC) is one of the most common malignant tumors of the digestive tract. Even after surgical resection and standardized treatment, the recurrence rate and metastasis rate of this tumor remain high. Therefore, prognostic prediction of the clinical outcome of HCC patients is still a challenge for clinicians (1,2). Although studies have suggested using different histological parameters to predict the prognosis of liver cancer cases, the new cancer classification system (3) that uses molecular markers to interpret the prognosis of liver cancer patients has broad prospects.

lncRNAs play an important role in cancer research as they are involved in many aspects in the biological activity of tumors, such as transcription, epigenetic regulation, and mRNA expression, and are reported to play a suppressive role in breast as well as other cancers (4,5). They may form pathways by interacting with miRNAs or mRNAs in human cancers. For example, lncRNA OIP5-AS1 was found to interact with miR-186a to inhibit ZEB1 expression in HCC which impaired tumor cell metastasis, and lncRNA HOXA-AS2 was found to suppress endothelium inflammation by regulating the activity of NF- κ B signaling (6,7). In the present study, lncRNA ZNF385D-AS2 was selected for research. lncRNA ZNF385D-AS2 may exert a regulatory function in various types of diseases and could regulate biological activities. Recently, lncRNA ZNF385D-AS2 has been suggested as a biomarker of novel stage in colorectal cancer progression although definite research is limited; however, whether

Correspondence to: Dr Yahui Liu, Department of General Surgery, The First Hospital of Jilin University, 71 Xinmin Street, Changchun, Jilin 130021, P.R. China
E-mail: liuyahui2018@yeah.net

Dr Fangfang Chen, Gastrointestinal Colorectal and Anal Surgery, China-Japan Union Hospital of Jilin University, 126 Xiantai Street, Changchun, Jilin 130033, P.R. China
E-mail: cff@jlu.edu.cn

Key words: liver cancer, lncRNA ZNF385D-AS2, prognosis, diagnosis

ZNF385D-AS2 could also be a specific marker in liver cancer remains to be elucidated.

The aim of this study was to identify the pathological roles of ZNF385D-AS2 in liver cancer. In the present study, through a retrospective analysis of data from The Cancer Genome Atlas-Liver Hepatocellular Carcinoma (TCGA-LIHC) cohort and tissue chip data (GEO-GSE54236), we evaluated the potential prognostic significance of ZNF385D-AS2 in patients with liver cancer and assessed the independent prognostic value of ZNF385D-AS2 expression for overall survival of liver cancer patients. Then, Gene Set Enrichment Analysis (GSEA) was performed to gain further insight into the biological functions and proteins related to the ZNF385D-AS2 regulatory mechanism. Co-expression and ceRNA predictive analysis methods were performed to obtain 59 gene sets most closely related to ZNF385D-AS2. Finally, we also used tissue chip data (GEO-GSE54236) to analyze functional enrichment and enriched ZNF385D-AS2 targets for consistent upregulated and downregulated gene sets, using Circos plots to reveal them.

Materials and methods

Data acquisition and collection. The data of liver cancer patients and RNA-seq expression results were downloaded with RCTCGA Toolbox package in R (version 3.5.3) (8). The gene microarray with cancer tissue data (GSE54236) (9,10) was downloaded from the GEO database (<https://www.ncbi.nlm.nih.gov/geo/>) (11).

Statistical analyses. SPSS software 23.0 (IBM Corporation, Armonk, NY, USA) was used for data analysis. Boxplots were used for discrete variables to measure the expression differences, and Chi-square tests were used to examine the correlation between ZNF385D-AS2 expression and clinical data (12). Receiver-operating characteristic curve (ROC) was drawn by 'p-ROC package' to evaluate the capability of diagnosis. We divided patients into high and low ZNF385D-AS2 expression groups using the optimal cutoff value of overall survival (OS) as determined by the Youden index. Kaplan-Meier curves were used to compare the differences in the OS and relapse-free survival (RFS) by using survival package in R (13). Univariate Cox analysis was used to select the related variables. Then, multivariate Cox analysis was applied for the influence of ZNF385D-AS2 expression on OS and RFS of the patients (14).

Gene set enrichment analysis (GSEA). GSEA is a computational method that determines whether an *a priori* defined set of genes shows statistically significant concordant differences between two biological states. In this study, GSEA was performed by using GSEA software 3.0 from the Broad Institute (UC San Diego, San Diego, CA, USA) (<http://software.broadinstitute.org/gsea/index.jsp>) (15). The gene expression data were RNA-seq data from TCGA-LIHC and GEO database. The gene set of 'c2.cp.biocarta.v6.2.symbols.gmt', 'c3.cp.biocarta.v6.2.symbols.gmt', 'c5.cp.biocarta.v6.2.symbols.gmt' and 'h.all.v6.2.symbols.gmt', which summarizes and represents specific, well-defined biological states or processes, was downloaded from the Molecular Signatures Database (<http://software.broadinstitute.org/gsea/msigdb/index.jsp>) (15).

The normalized enrichment score (NES) was acquired by analyzing with permutations for 1,000 times. A gene set was considered to be significantly enriched at a normal P-value <0.05 and false discovery rate (FDR) <0.25.

Gene enrichment and functional annotation evaluation. The Database for Annotation, Visualization, and Integrated Discovery (DAVID; <http://david.abcc.ncifcrf.gov/>) and KO-Based Annotation System (KOBAS) (<http://kobas.cbi.pku.edu.cn/>) were used to conduct relevant pathway analysis (16,17), and Gene Ontology (GO) analysis was performed for the functional annotation of the predicted genes (17). Three GO terms [biological process (BP), cellular component (CC) and molecular function (MF)] were utilized to identify the enrichment of target genes. In addition, Kyoto Encyclopedia of Genes and Genomes (KEGG) pathway analysis was performed for the functional annotation of these genes. GO terms and KEGG pathway with P-values <0.05 were considered statistically significant. The enrichment map of annotation analysis was drawn using Cytoscape (version 3.3.1) (<http://www.cytoscape.org/cy3.html>) and R (version 3.5.3).

Co-expression genes and ceRNA pattern predictive analysis. In order to analyze the specific functions of lncRNA ZNF385D-AS2, it was necessary to analyze the interaction between lncRNAs and the coding genes as well as the interacting miRNAs (18). Based on data from the TCGA-LIHC and GEO (GSE54236) databases, using the Pearson and Spearman correlation analysis based on the Logistic function ('WGCNA' package in R), the co-expression relationship between ZNF385D-AS2 and the coding genes and miRNAs were identified, and the co-expression network between ZNF385D-AS2 and the coding genes and miRNAs were mapped in Cytoscape. At the same time, comparative analysis of several lncRNA databases, such as NONCODE (<http://www.noncode.org/>), lncRBase (<http://starbase.sysu.edu.cn/>), Co-lncRNA (<http://www.biobigdata.com/Co-lncRNA/>), was carried out to identify the miRNAs that exhibited regulatory relationships with ZNF385D-AS2 and mRNAs which these miRNAs may regulate. After comparing the data from the TCGA and GEO databases, the possible ceRNA patterns in HCC were predicted and plotted which were also mapped in Cytoscape. Circos plots was generated based on the remappings from these two predicted results. Circos plots were generated using the Circos visualization tool in R ('RCircos' package in R) (19).

Results

Patient characteristics. Both gene expression and clinical data of patients with liver cancer were downloaded from The Cancer Genome Atlas (TCGA-LIHC) database (9,10). The total number of patients was 427. After initial screening, we omitted 13 normal samples and 74 tumor samples with missing or unclear information, and the remaining 303 tumor samples and 37 normal samples were available. The detailed clinical characteristics, including age, sex, TNM stage, survival status, pathological status, and ethnic compositions are shown in Table I.

Table I. Demographic and clinical characteristics of the The Cancer Genome Atlas-Liver Hepatocellular Carcinoma (TCGA-LIHC) cohort (N=303).

Characteristics	Number of samples, n (%)	
	n	Percentage (%)
Age (years)		
≤55	107	35.31
>55	196	64.69
Sex		
Female	92	30.36
Male	211	69.64
T stage		
T1	153	50.50
T2	76	25.08
T3	63	20.79
T4	10	3.30
Unknown	1	0.33
M stage		
M0	229	75.78
M1	3	0.99
Mx	71	23.43
N stage		
N0	220	72.61
N1	3	0.99
Nx	80	26.40
Stage		
I	153	50.50
II	74	24.42
III	72	23.76
IV	4	1.32
Histologic grade		
G1	42	13.86
G2	144	47.52
G3	105	34.65
G4	12	3.96
Vital status		
Living	217	71.62
Deceased	86	28.38
Race		
Asian	150	49.50
Black	8	2.64
Caucasian	139	45.87
Unknown	6	1.98
ZNF385D-AS2 expression		
Low	184	60.73
High	119	39.27
Total	303	100

Low expression of lncRNA ZNF385D-AS2 in HCC. Using boxplots, we measured the differences in ZNF385D-AS2 expression in liver cancer patients and control subjects. As shown in Fig. 1A, we evaluated the overall expression trend of

ZNF385D-AS2 in liver cancer, then found that ZNF385D-AS2 expression was significantly lower in primary HCC tissues than that in normal liver tissues ($P<0.001$). Moreover, as shown in Fig. 1A-K, there was differential ZNF385D-AS2 expression in the groups according to sex ($P=0.046$; Fig. 1C), vital status ($P=0.037$; Fig. 1D), clinical stage ($P=0.001$; Fig. 1E), T stage ($P=0.001$; Fig. 1F) and survival time ($P=0.033$; Fig. 1K). Of note, differences in ZNF385D-AS2 expression were observed according to patient age as well as the TNM stage of cancer, and clinicopathological parameters (Fig. 1). We also collected data on the expression of ZNF385D-AS2 in several common digestive tumors based on TCGA database. After horizontal comparison, we found that except for cholangiocarcinoma and rectal cancer, the expression of ZNF385D-AS2 was reduced in most digestive system tumors (Fig. 2).

Correlation between ZNF385D-AS2 expression and clinical features of the HCC samples. According to Chi-square tests, the correlation between the clinical features and the expression of ZNF385D-AS2 was analyzed and is documented in Table II. The expression of ZNF385D-AS2 was highly associated with sex ($\chi^2=3.846$, $P=0.050$), T stage ($\chi^2=3.875$, $P=0.049$), M stage ($\chi^2=4.221$, $P=0.040$), N stage (Fisher's exact test, $P<0.001$) and clinical stage ($\chi^2=4.365$, $P=0.037$).

Low ZNF385D-AS2 expression is an independent prognostic factor for poor survival. We generated Kaplan-Meier curves of overall survival (OS), and log-rank tests showed that ZNF385D-AS2 low-expression was associated with poor OS ($P=0.0079$; Fig. 3A). Further subgroup analysis (Fig. 3A-O) showed that ZNF385D-AS2 low-expression was associated with the poor OS of patients with sex (male) ($P=0.015$; Fig. 3D), M0 stage ($P=0.0099$; Fig. 3H), N0 stage ($P=0.028$; Fig. 3I), age ≤ 55 ($P=0.023$; Fig. 3J), early pathological stage (G1/2) ($P=0.044$; Fig. 3L) and race (Asian) ($P=0.0046$; Fig. 3N).

As shown in Fig. 4, the ROC of ZNF385D-AS2 was executed, and the area under the curve (AUC) was 0.594, which represented moderate diagnostic ability.

In ZNF385D-AS2 low-expression patients, we used univariate analysis and selected the critical variables including age, sex, clinical stage, pathological grade and TMN classification. Multivariate analysis with the Cox proportional hazards model indicated that clinical stage (HR=1.418, $P=0.011$) and T classification (HR=1.713, $P<0.001$) were independent prognostic factors for patients with HCC (Table III).

GSEA identifies the biological functions and proteins associated with ZNF385D-AS2. To identify the biological functions activated in liver cancer, we conducted GSEA between high and low ZNF385D-AS2 expression data sets. GSEA revealed significant differences (FDR <0.25 , $P<0.05$) in the enrichment of 'MSigDB Collection', and the specific contents are shown in Table IV. In the nucleus, 'histone deubiquitination', 'V-D-J recombination' and 'translation factor activity RNA binding' were found to be differentially enriched in the ZNF385D-AS2 low-expression phenotype. Meanwhile, Table IV shows that 'cytoplasmic exosome RNase complex', 'nuclear exosome RNase complex', 'retrograde transport endosome to Golgi' and 'Golgi organization' exhibited a positive correlation with ZNF385D-AS2. In the

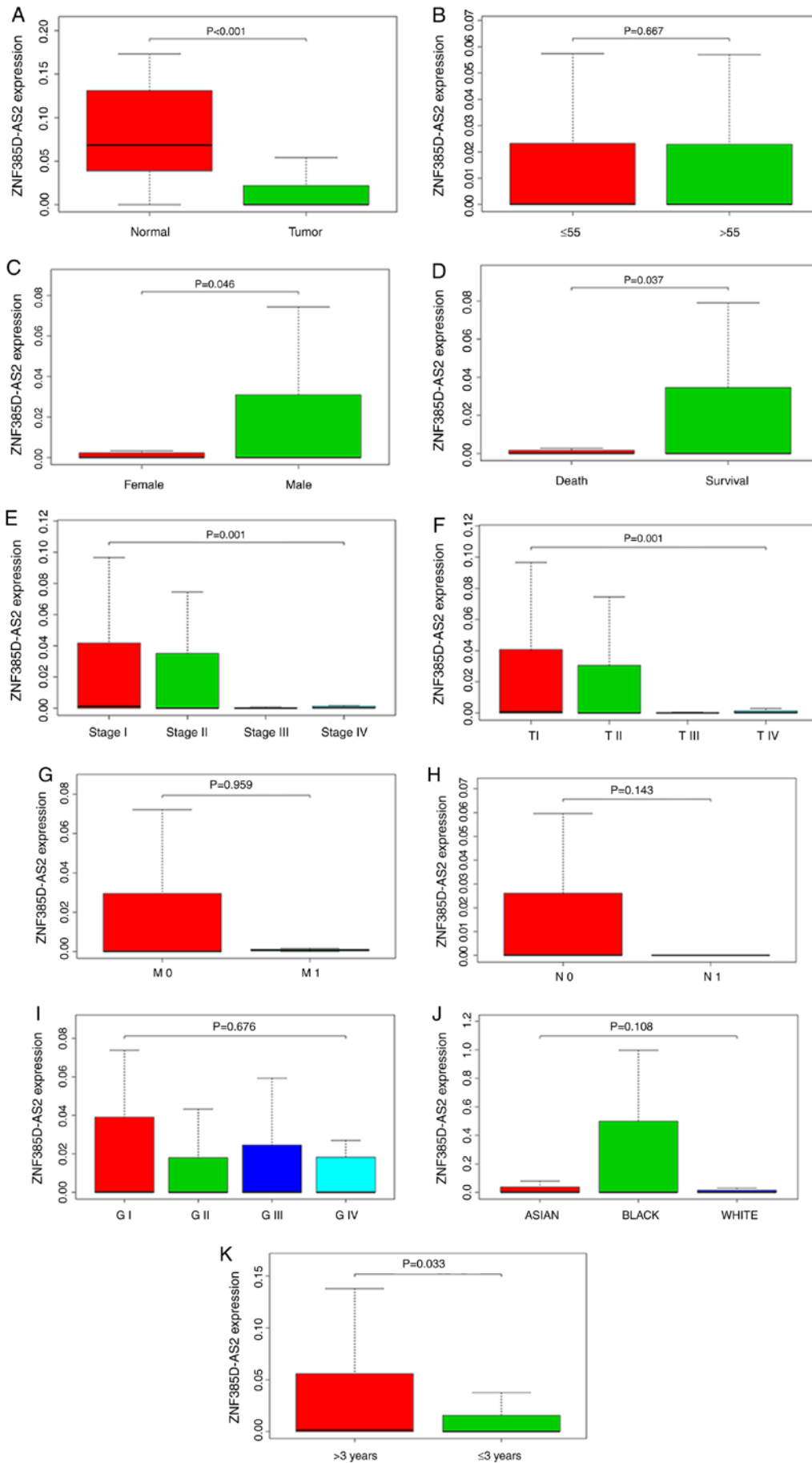


Figure 1. Boxplots showing differences in ZNF385D-AS2 expression according to tissue type (A), patient age (≤55 vs. >55 years) (B), sex (C) and survival status (D) as well as clinical stage (E), TNM stage (F-H), pathological status (I), race (J) and survival time (>3 vs. ≤3 years) (K). lncRNA ZNF385D-AS2, long non-coding RNA zinc finger protein 385D antisense RNA 2.

Table II. Correlation of lncRNA ZNF385D-AS2 expression in HCC tissues and clinicopathologic variables of the HCC samples (N=303).

Clinical characteristics	Variables	No. of patients	ZNF385D-AS2 expression		χ^2	P-value
			High, n	Low, n		
Age (years)	≤55	107	53	54	0.006	0.938
	>55	196	98	98		
Sex	Female	92	38	54	3.846	0.050
	Male	211	113	98		
T stage	T1	153	84	69	3.875	0.049
	T2	76	36	40		
	T3	63	23	40		
	T4	10	7	3		
M stage	M0	229	107	122	4.221	0.040
	M1	3	2	1		
	Mx ^a	71	42	29		
N stage	N0	220	106	114	<0.001^b	
	N1	3	0	3		
	Nx ^a	80	34	46		
Grade	G1	42	24	18	2.038	0.564
	G2	144	69	75		
	G3	105	47	58		
	G4	12	5	7		
Stage	Stage I/II	227	121	106	4.356	0.037
	Stage III/IV	76	30	46		
Fustat	Surviving	217	102	115	3.055	0.081
	Deceased	86	50	36		
Race	Asian	150	77	73	0.004	0.950
	Other race	147	76	71		

Bold P-values indicate statistically significant correlations ($P \leq 0.05$). ^aNot included in the analysis. ^bFisher's exact test. HCC, hepatocellular carcinoma.

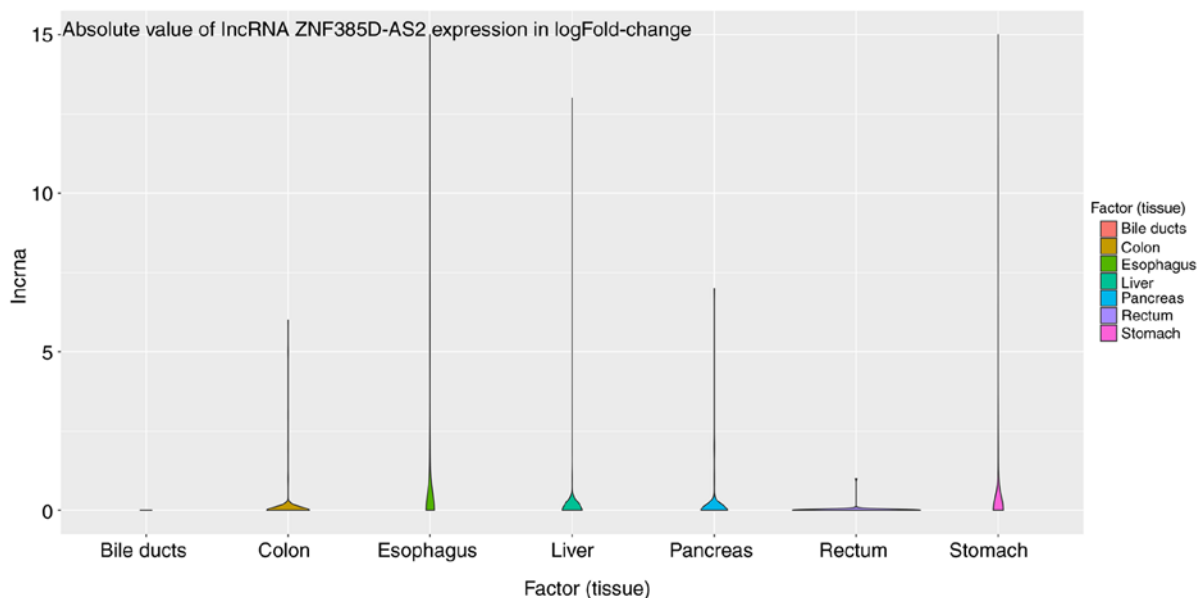


Figure 2. lncRNA ZNF385D-AS2 expression in several common digestive system tumors based on TCGA database. The expression level of ZNF385D-AS2 in tumors was found to be lower than that in the normal tissues. The result data is logarithmically processed and its absolute value is calculated. lncRNA ZNF385D-AS2, long non-coding RNA zinc finger protein 385D antisense RNA 2.

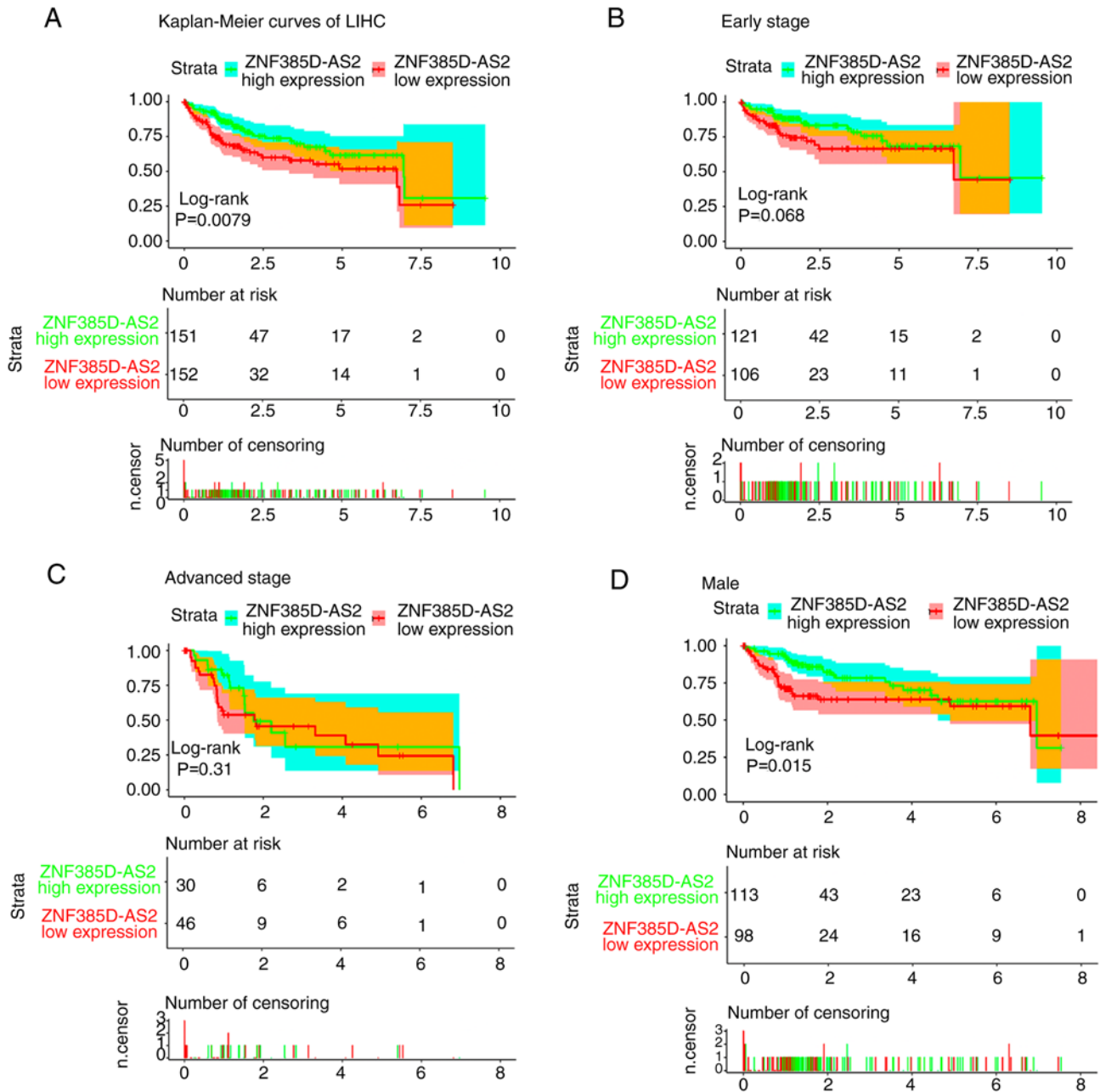


Figure 3. Kaplan-Meier curves for survival of HCC patients according to ZNF385D-AS2 expression in HCC tissues. Patients were divided into high and low ZNF385D-AS2 expression groups using the median value of ZNF385D-AS2 expression as the cut-off point. (A) Kaplan-Meier curves of overall survival (OS), and log-rank tests showed that ZNF385D-AS2 low-expression was associated with poor OS. Survival analysis and subgroup analysis according to clinical stage (B and C) and male sex (D) were performed based on Kaplan-Meier curves. HCC, hepatocellular carcinoma; lncRNA ZNF385D-AS2, long non-coding RNA zinc finger protein 385D antisense RNA 2.

cytoplasm, low expression of ZNF385D-AS2 was also related to various cytological behaviors such as ‘protein transport along microtubule’, ‘negative regulation of defense response to virus’ and ‘oxidoreductase activity acting on the CNH group of donors NAD⁺ or NADP⁺ as acceptor’. Moreover, Table IV shows that as the expression of ZNF385D-AS2 is decreased, various intracellular signaling pathways are also affected. These signaling pathways encompass the metabolic synthesis and degradation of substances, such as ‘one carbon pool by folate’, ‘glyoxylate and dicarboxylate metabolism’, ‘fatty acid metabolism’, ‘selenoamino acid metabolism’, ‘fructose and mannose metabolism’ as well as ‘aminoacyl tRNA biosynthesis’, ‘glycosyl-phosphatidylinositol GPI

anchor biosynthesis’, ‘RNA degradation’ and ‘lysine degradation’. Moreover, it also affects signal transfer and material transport within HCC cells, including ‘ABC transporters’, ‘Snare interactions in vesicular transport’ and ‘basal transcription factors’, in addition to the progression of various diseases, including ‘acute myeloid leukemia’, ‘hepatitis’ and ‘endometrial cancer’.

During the progression of liver cancer, the expression of ZNF385D-AS2 was found to gradually decrease. In this process, expression levels of a certain number of mRNAs were found to be altered as ZNF385D-AS2 decreased, and these results are summarized in Table V. The expression levels of MEK, EGFR, ERB2, mTOR initially increased and then decreased. A positive

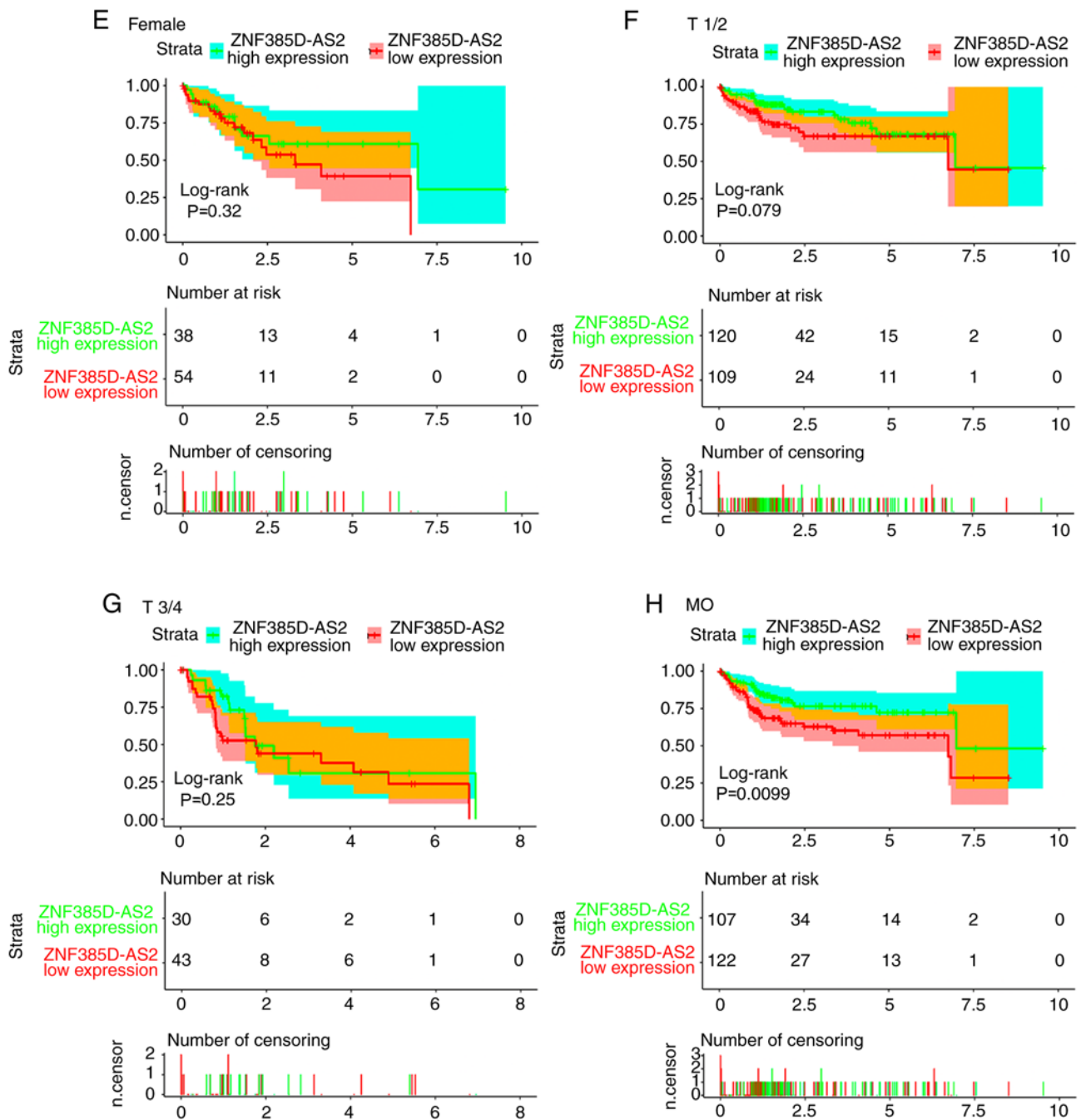


Figure 3. Continued. Patients were divided into high and low ZNF385D-AS2 expression groups using the median value of ZNF385D-AS2 expression as the cut-off point. Survival analysis and subgroup analysis according to female sex (E) and TNM stage (F-H) were performed based on Kaplan-Meier curves. lncRNA ZNF385D-AS2, long non-coding RNA zinc finger protein 385D antisense RNA 2.

regulation relationship was found between the expression levels of ZNF385D-AS2 and GLI1, CAMP, cyclin D1, Wnt. However, there still exists a negative regulatory relationship between the expression level of JAK2, PDGF-ERK and BRCA1. It is worth noting that P53, a gene that inhibits the development of cancer, was found to first decrease and then increase as the amount of ZNF385D-AS2 expression decreases.

Prediction of related genes and functional annotation analyses. We next used R's 'edgr' package to calculate the difference (log fold-change >1, P<0.05) in expression between mRNAs, miRNAs and lncRNAs in the TCGA-LIHC and

GEO (GSE54236) databases. Then we conducted comparative analysis of several lncRNA databases, such as NONCODE, LncRBase, Co-LncRNA to identify miRNAs that have regulatory relationships with ZNF385D-AS2 and mRNAs that these miRNAs may regulate. After comparing the data from the TCGA and GEO databases, the possible ceRNA patterns in HCC were predicted and plotted in Cytoscape (Fig. 5A). At the same time, we used Pearson and Spearman correlation analysis based on the Logistic function ('WGCNA' package in R), of the co-expression relationship between ZNF385D-AS2. The mRNAs and miRNAs were identified, and the co-expression network between ZNF385D-AS2 and

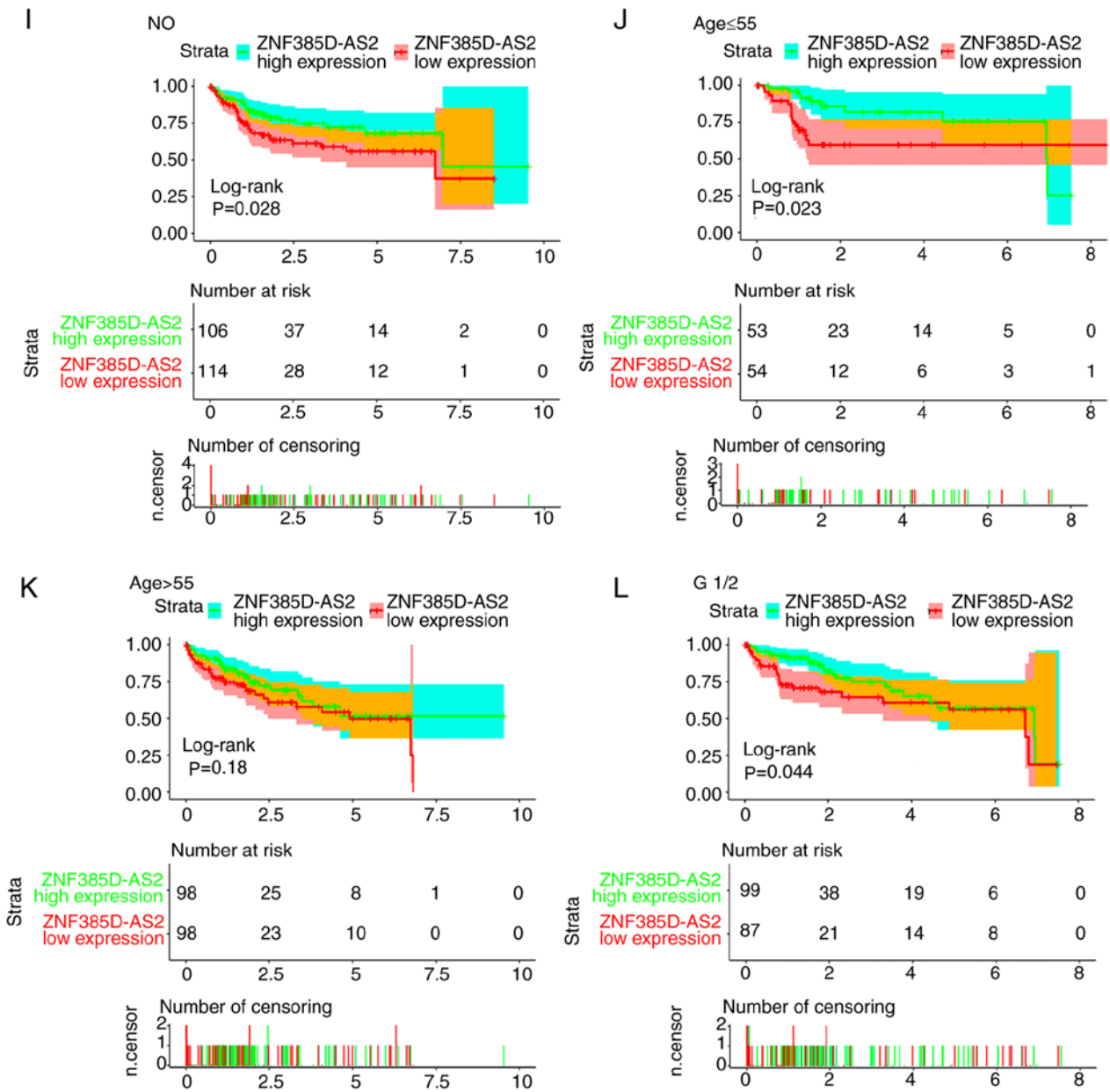


Figure 3. Continued. Patients were divided into high and low ZNF385D-AS2 expression groups using the median value of ZNF385D-AS2 expression as the cut-off point. Survival analysis and subgroup analysis according to TNM stage (continued) (I), age (J and K) and pathological status (L) were performed based on Kaplan-Meier curves. lncRNA ZNF385D-AS2, long non-coding RNA zinc finger protein 385D antisense RNA 2.

the mRNAs and miRNAs was also mapped (Fig. 5B). The result strongly suggested that there is a regulatory signaling axis that exists between ZNF385D-AS2 and miR-96 and miR-182.

We then integrated the regulatory networks obtained by these two different methods, and again performed GO terms and KEGG pathway analyses for these mRNAs after removal of the duplicates. Cytoscape was used to conduct an analysis map of genes enriched in the GO terms and to construct an interaction network for the related genes (Fig. 6A). As shown in Fig. 6B and C, these specific mRNAs were most highly enriched in the following GO terms: Molecular function (MF) (growth factor activity, transforming growth factor β receptor binding), biological process (BP) (axon guidance, cell development, regulation of MAPK cascade, positive regulation of cell division, positive regulation of pathway-restricted SMAD

protein phosphorylation, cell growth, SMAD protein signal transduction) and cellular component (CC) (extracellular space). Based on the results in Fig. 5, we used R to perform a dot-enrichment of the KEGG pathway obtained from KOBAS. These signaling pathways are able to affect material metabolism within HCC cells, signal transduction, progression of various diseases, and other biological behaviors (Fig. 7).

Co-expression and ceRNA pattern regulated genome maps. Alignments of gene co-expression maps to GRCh38.95 identified reference genomic regions contributing to the composition of 59 genome sets. According to the co-expressing genes and ceRNA regulatory network predictive analysis results, we comprehensively analyzed the gene co-expression result and ceRNA regulatory network in GEO (GSE54236) and TCGA-LICH with ZNF385D-AS2. In order to find the most

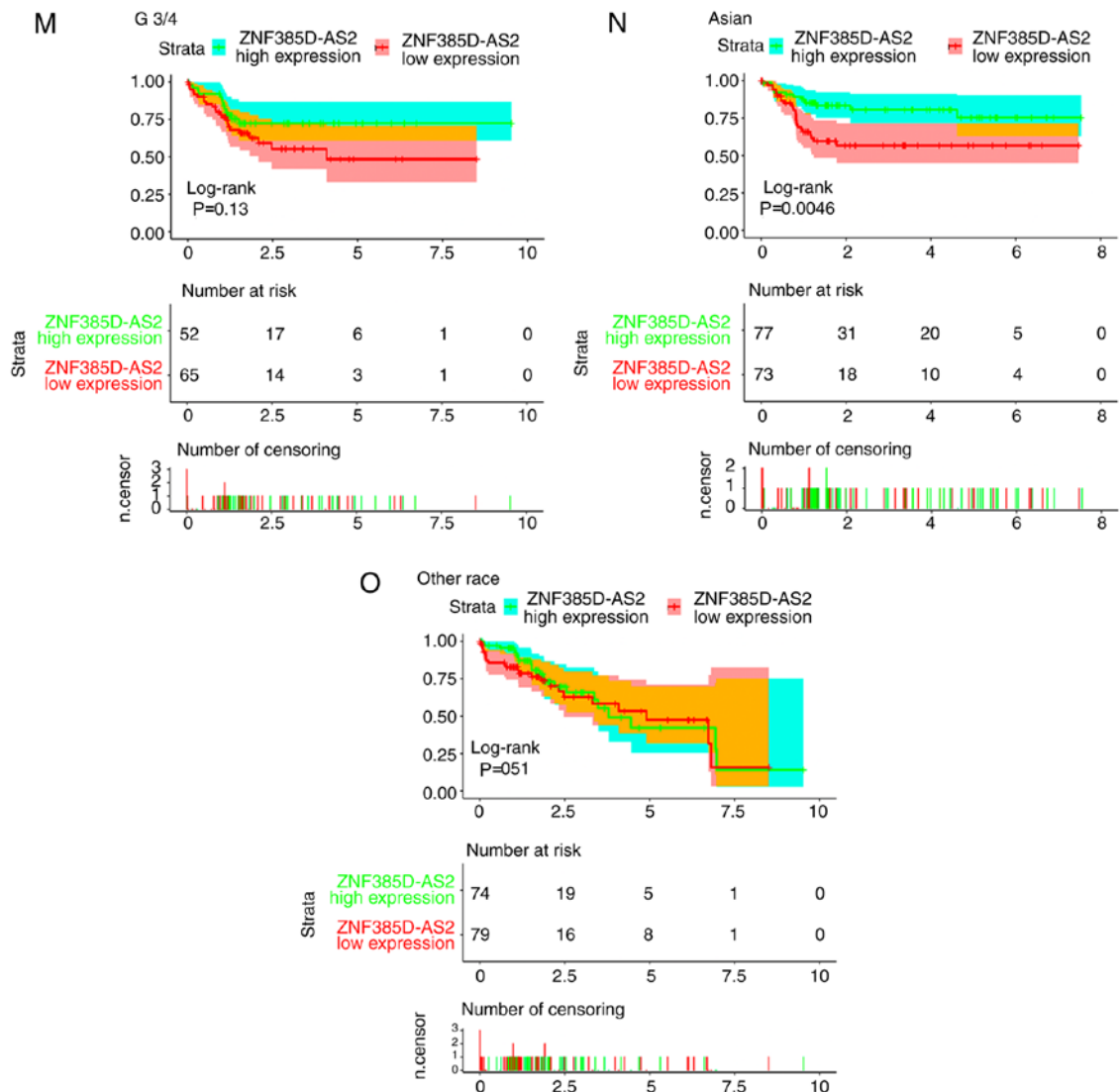


Figure 3. Continued. Patients were divided into high and low ZNF385D-AS2 expression groups using the median value of ZNF385D-AS2 expression as the cut-off point. Survival analysis and subgroup analysis according to pathological status (continued) (M), and race (N and O) were performed based on Kaplan-Meier curves. lncRNA ZNF385D-AS2, long non-coding RNA zinc finger protein 385D antisense RNA 2.

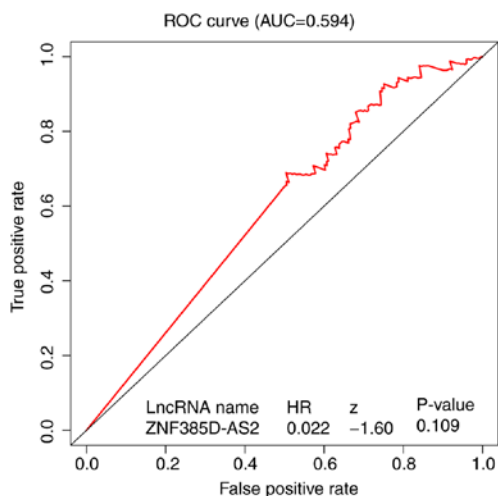


Figure 4. ROC curve to identify the optimal cut-off value for dividing patients into high and low ZNF385D-AS2 expression groups. AUC, area under the curve; ROC, receiver-operating characteristic curve. HR, hazard ratio; lncRNA ZNF385D-AS2, long non-coding RNA zinc finger protein 385D antisense RNA 2.

represented reference fragments, all GRCh38.95 loci present in the gene co-expressed maps were deduced and merged, resulting in 59 reference donor fragments, which settled in the outermost track. The numbers of gene co-expressed maps containing each of these fragment labels were then marked in the second track, excluding duplicate counts. We found 96 pairs of genes which existed in a co-expressed phenomenon. In the inner sector, we linked these pairs of gene sets that had co-expression relationships with lines. The sum of gene co-expressed map alignments across the whole genome was used as the links for the 59 gene co-expressed maps in the Circos plot (Fig. 8).

Discussion

lncRNAs, as a group of genes, have been reported to be highly or lowly expressed in cancers. Furthermore, lncRNAs may serve as oncogenes, promoting the development of cancer by interacting with miRNAs and mRNAs to regulate cytological behavior (20). As demonstrated by this research, lncRNA

Table III. Univariate and multivariate analyses of OS in patients with liver cancer with low expression of lncRNA ZNF385D-AS2.

Parameters	Univariate analysis			Multivariate analysis		
	HR	95% CI	P-value	HR	95% CI	P-value
Age, years (≤ 55 vs. > 55)	1.361	0.991-1.041	0.243			
Sex (female vs. male)	0.691	0.419-1.476	0.681			
Race (Asian vs. Black and Caucasian)	0.988	0.449-0.991	0.32			
Grade (G1 and G2 vs. G3 and G4)	0.044	0.722-1.612	0.835			
Stage (Stage I and II vs. III and IV)	1.813	1.257-2.405	0.013	1.418	0.926-2.452	0.011
T stage (T1 and T2 vs. T3 and T4)	2.299	1.594-3.401	<0.001	1.713	1.269-3.120	<0.001
M stage (M0 vs. M1)	2.282	1.994-2.407	0.059			
N stage (N0 vs. N1)	1.119	1.063-1.376	0.073			

Bold P-values indicate statistical significance ($P < 0.05$). OS, overall survival; HR, hazard ratio; CI, confidence interval.

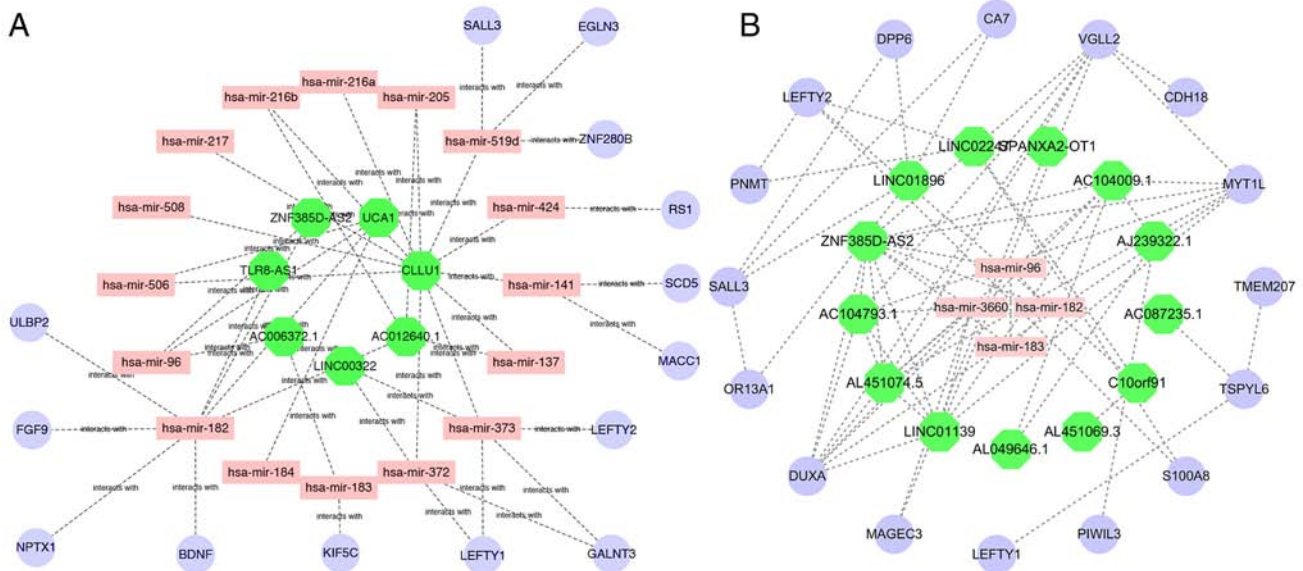


Figure 5. Possible ceRNA regulatory and co-expression networks. (A) After comparing several lncRNA databases, the possible ceRNA patterns in HCC were predicted and plotted in Cytoscape. (B) Using the ‘WGCNA’ package in R, a possible co-expression regulatory network was mapped. The results highly suggest that there is a regulatory signaling axis between ZNF385D-AS2 and miR-96 and miR-182. ceRNA, competing endogenous RNA; HCC, hepatocellular carcinoma; lncRNA ZNF385D-AS2, long non-coding RNA zinc finger protein 385D antisense RNA 2.

ZNF385D-AS2 plays an important role in HCC and can be used as a biomarker to monitor liver cancer prognosis. After analyzing the ZNF385D-AS2 expression in liver cancer patient samples, we found factors that are correlated with ZNF385D-AS2 low-expression, namely, sex, vital status, clinical stage, T stage and survival time.

Much research has been conducted in recent years concerning the role played by ZNF385D-AS2 in common digestive tumors where ZNF385D-AS2 was found to be downregulated (21). Recently, it has been suggested that down-regulation of ZNF385D-AS2 is involved in cancers including gastric cancer and human non-small cell lung cancer (NSCLC) although there is limited research to confirm this. Based on the present study, ZNF385D-AS2 low-expression was observed in liver cancer, consistent with the same ZNF385D-AS2 low-expression state concerning other types of tumors in the

TCGA database. It is notable that ZNF385D-AS2 expression gradually decreased from T1 to T4 and from clinical stage I to clinical stage IV, suggesting its relevance in the progression of liver cancer. In addition, ZNF385D-AS2 expression was higher in male patients than female patients, suggesting its relevance to sex and the necessity to perform subgroup analysis. Especially in patients with a survival time of less than 3 years, this difference in expression was more pronounced. Moreover, low expression of ZNF385D-AS2 was associated with survival status, making it necessary to explore its link with survival. After analyzing the M and N stages of liver cancer, although the results did not achieve statistical significance, the expression level of ZNF385D-AS2 in M1 and N1 phase was lower than that in M0 and N0 phase.

Some previous studies also analyzed the way ZNF385D-AS2 affects the occurrence and development of

Table IV. lncRNA ZNF385D-AS2 low-expression related GO terms and KEGG pathways in HCC.

GO Terms	Size	ES	NES	NOM P-value
GO_DEOXYRIBONUCLEOSIDE_TRIPHOSPHATE_METABOLIC_PROCESS	16	0.6713025	1.8666009	<0.001
GO_HISTONE_MRNA_METABOLIC_PROCESS	28	0.5867406	1.8163215	0.010204081
GO_TRANSLATION_FACTOR_ACTIVITY_RNA_BINDING	83	0.3732794	1.7212093	0.030425964
GO_SOMATIC_CELL_DNA_RECOMBINATION	33	0.6081087	1.7152647	0.0078125
GO_V_D_J_RECOMBINATION	16	0.7184384	1.7132919	<0.001
GO_OXIDOREDUCTASE_ACTIVITY_ACTING_ON_THE_CH_NH_GROUP_OF_DONORS_NAD_OR_NADP_AS_ACCEPTOR	18	0.6175537	1.7093326	0.010162601
GO_EXOSOME_RNASE_COMPLEX	21	0.5698847	1.6803491	0.024340771
GO_TELOMERASE_HOLOENZYME_COMPLEX	19	0.5726633	1.6542872	0.017928287
GO_MICROTUBULE_NUCLEATION	18	0.5810587	1.6540635	0.035781544
GO_SOMATIC_DIVERSIFICATION_OF_IMMUNE_RECEPTORS	41	0.5348539	1.6465995	0.033663366
GO_NUCLEAR_LOCALIZATION_SEQUENCE_BINDING	20	0.6116292	1.6374387	0.019880716
GO_NUCLEAR_LOCALIZATION_SEQUENCE_BINDING	18	0.4993185	1.6094043	0.042307694
GO_NEGATIVE_REGULATION_OF_DEFENSE_RESPONSE_TO_VIRUS	15	0.5706286	1.6084776	0.03206413
GO_CYTOPLASMIC_EXOSOME_RNASE_COMPLEX	22	0.5604809	1.5993211	0.05668016
GO_SNRNA_PROCESSING	71	0.3641102	1.5988086	0.05078125
GO_RETROGRADE_TRANSPORT_ENDOSOME_TO_GOLGI	27	0.5950033	1.5972574	0.038910504
GO_PROTEIN_TRANSPORT_ALONG_MICROTUBULE	16	0.5016319	1.5902865	0.060546875
GO_PRE_AUTOPHAGOSOMAL_STRUCTURE_MEMBRANE	84	0.3968728	1.5886257	0.05668016
GO_GOLGI_ORGANIZATION	15	0.5812139	1.5849311	0.037254903
GO_NUCLEAR_EXOSOME_RNASE_COMPLEX	21	0.5922844	1.5812734	0.035785288
GO_HISTONE_DEUBIQUITINATION				
KEGG Pathways	Size	ES	NES	NOM P-value
KEGG_ONE_CARBON_POOL_BY_FOLATE	17	0.5607268	1.6354854	0.02028398
KEGG_RNA_DEGRADATION	57	0.383115	1.6217419	0.04722793
KEGG_GLYOXYLATE_AND_DICARBOXYLATE_METABOLISM	16	0.5347747	1.4103469	0.10763209
KEGG_ABC_TRANSPORTERS	44	0.4471579	1.2647074	0.16201118
KEGG_LYSINE_DEGRADATION	44	0.417074	1.318973	0.21428572
KEGG_SNARE_INTERACTIONS_IN_VESICULAR_TRANSPORT	37	0.3300203	1.2587498	0.21875
KEGG_AMINOACYL_TRNA_BIOSYNTHESIS	41	0.3709021	1.1858624	0.3238289
KEGG_GLYCOSYLPHOSPHATIDYLINOSITOL_GPI_ANCHOR_BIOSYNTHESIS	25	0.3702377	1.155113	0.33463797
KEGG_GLYCOSAMINOGLYCAN_BIOSYNTHESIS_KERATAN_SULFATE	15	0.4000842	1.1251451	0.33675563
KEGG_BASAL_TRANSCRIPTION_FACTORS	32	0.3257739	1.1036584	0.35135135
KEGG_PROXIMAL_TUBULE_BICARBONATE_RECLAMATION	23	0.4029235	1.0807126	0.35238096
KEGG_MISMATCH_REPAIR	23	0.4058034	1.1521276	0.35966736
KEGG_NUCLEOTIDE_EXCISION_REPAIR	43	0.3010005	1.1056284	0.3783231
KEGG_SPLICEOSOME	125	0.2617425	1.0658554	0.39430895
KEGG_ACUTE_MYELOID_LEUKEMIA	57	0.2873536	1.0399672	0.3966597
KEGG_FATTY_ACID_METABOLISM	41	0.4589222	1.121886	0.41860464
KEGG_SELENOAMINO_ACID_METABOLISM	26	0.2914508	1.023621	0.42376238
KEGG_PEROXISOME	78	0.3360126	1.045031	0.4318182
KEGG_FRUCTOSE_AND_MANNANOSE_METABOLISM	34	0.2906978	0.9975369	0.45
KEGG_ENDOMETRIAL_CANCER	52	0.2653771	0.9771847	0.45436105

Enrichment Biological Functions from GSEA. HCC, hepatocellular cancer; GO, Gene Ontology; KEGG, Kyoto Encyclopedia of Genes and Genomes; GSEA, Gene Set Enrichment Analysis; ES, Enrichment Score; NES, Normalized Enrichment Score.

Table V. Enrichment of gene expression from GSEA.

Expression change	Gene name
Decreased expression	<i>JAK2, SIRNA, PDGF, BCAT, STK33, RB, TBK1, EIF4E, BRCA1</i>
Increased expression	<i>CSR, STK33, GLI1, CAMP, PIGF, EGFR, STK33, KRAS, TBK1, Cyclin D1, Wnt</i>
First increased then decreased	<i>VEGF, CSR, ESC, CRX, MTOR, MEK, EGFR, ERB2, LTE2, LEF1, GLI1, RAF, ATF2</i>
First decreased then increased	<i>HOXA9, RB, P53</i>

Notably, upon lncRNA ZNF385D-AS2 low-expression, the expression levels of other genes were found to be altered. GSEA, Gene Set Enrichment Analysis.

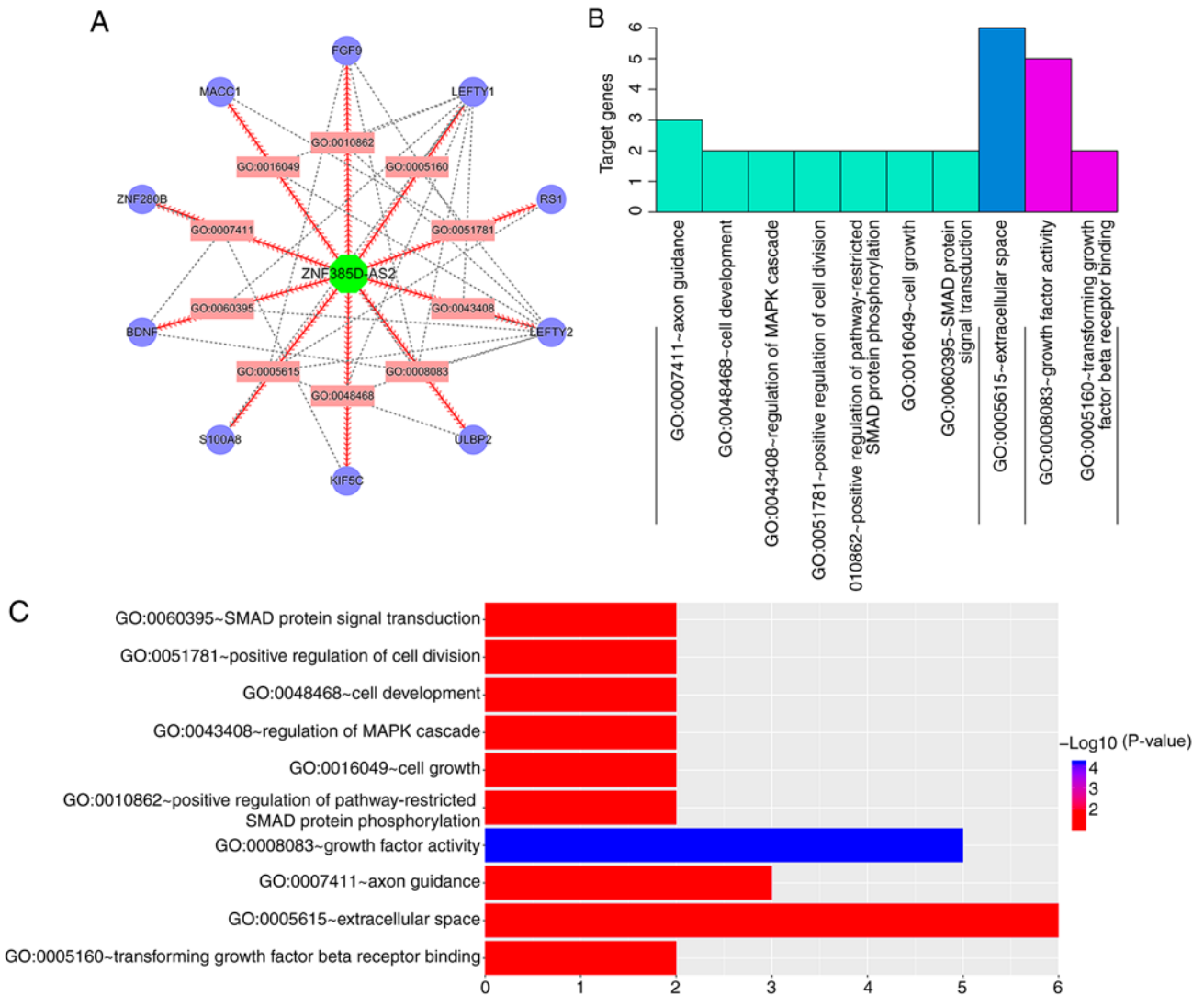


Figure 6. Significant GO terms identified by DAVID. (A) Cytoscape was used to conduct an analysis map of genes enriched in the GO terms and to construct an interaction network for the related genes. (B and C) mRNAs most highly enriched in the GO terms. GO, Gene Ontology. DAVID, Database for Annotation, Visualization and Integrated Discovery.

tumors (22). By large-scale clinical statistics, the obvious low-expression of ZNF385D-AS2 is found in many liver cell lines (23). In this study, ZNF385D-AS2 can affect the initiation and proliferation of tumor, which explains that it is clinically related to the TNM classification. ZNF385D-AS2 exhibits a strong association with cancer prognosis. In the present study, it was found that low expression of ZNF385D-AS2 indicated

a poor overall survival (OS), particularly in relation to age ≤ 55 years, sex (male), race (Asian), M0 stage, N0 stage as well as early histologic grade G1/G2. Cox analysis demonstrated the independent prognostic effect of ZNF385D-AS2 on the OS of patients; therefore, it can be used to monitor liver cancer as a biomarker. Some studies have also shown that in addition to affecting some of the common biological functions of tumor

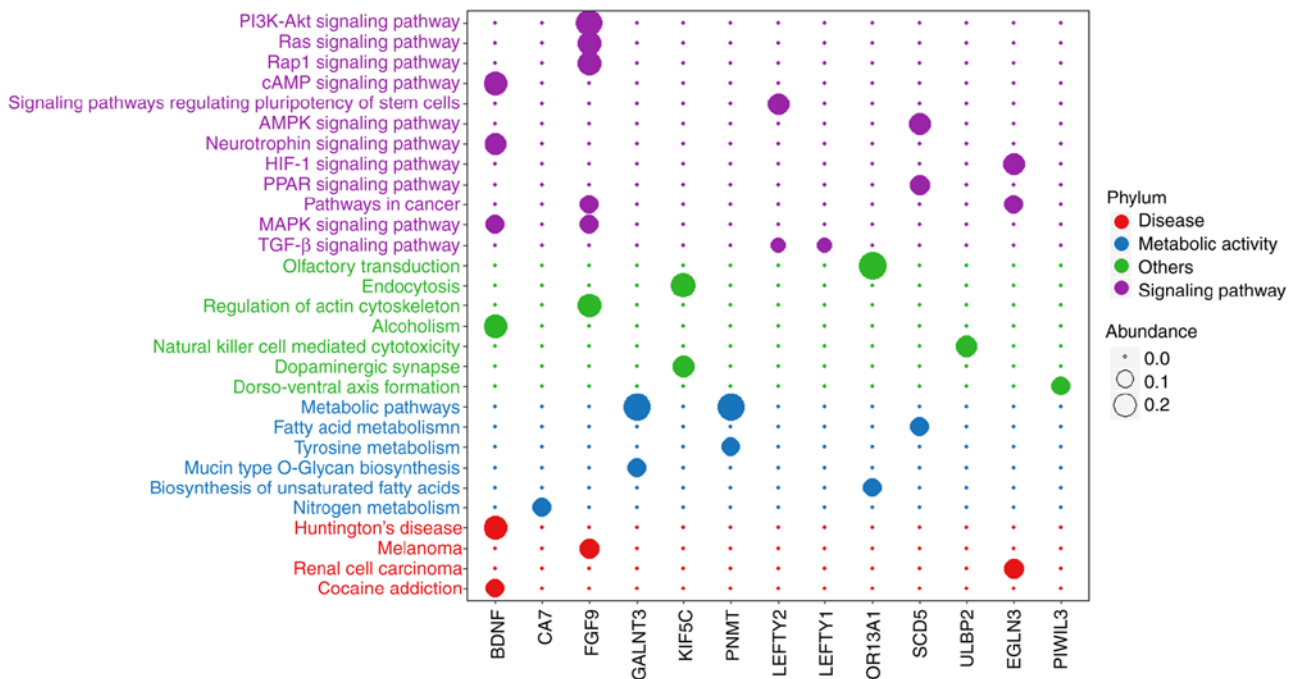


Figure 7. Significant KEGG pathways identified by KOBAS. Using the genes predicted in Fig. 5, 29 different KEGG pathways were found to be enriched. These signaling pathways were roughly divided into four broad categories, of which 13 genes were most correlated. KOBAS, KO-Based Annotation System. KEGG, Kyoto Encyclopedia of Genes and Genomes.

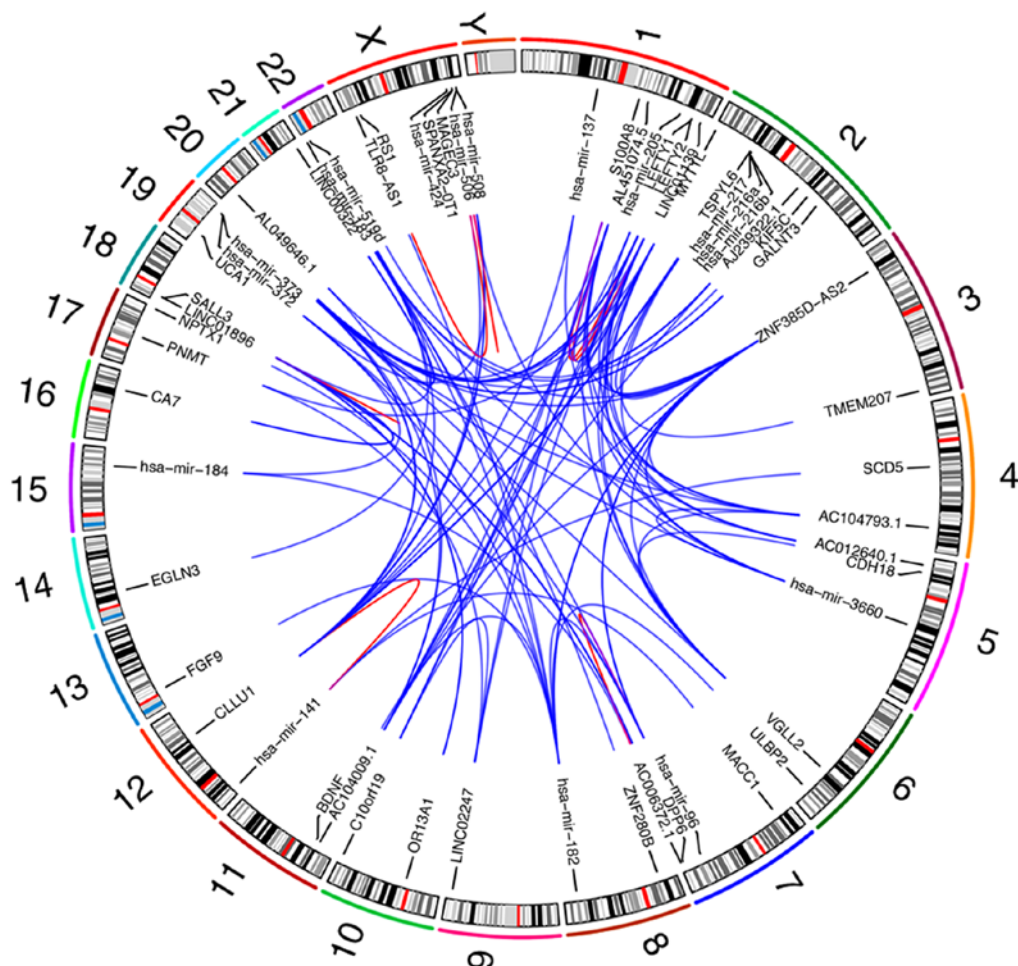


Figure 8. Circos plot derived from possible co-expression and ceRNA regulatory networks. Linked lines in the middle of the Circos plots show the relationship between each pair of co-expressed genes. The next track shows the labels of these genes. The outermost track shows the chromosome localization information of these genes. Plots were generated using the Circos visualization tool by R. ceRNA, competing endogenous RNA.

cells, lncRNA ZNF385D-AS2 can also affect some specific cytological behaviors although research is sparse confirming this. After functional enrichment analysis of ZNF385D-AS2, we found that ZNF385D-AS2 has a close relationship with the formation and efflux of exosomes. It is closely related to histone deubiquitination, V-D-J recombination and translation factor activity RNA binding, but also affects the regulation of defense response to virus, pre-autophagosomal membrane formation and as an acceptor acting on oxidoreductase activity. Not only that, but some of the intracellular signaling pathways are also affected. These signaling pathways encompass the metabolic synthesis and degradation of substances, such as 'one carbon pool by folate', 'glyoxylate and dicarboxylate metabolism', 'fatty acid metabolism', 'selenoamino acid metabolism', 'fructose and mannose metabolism' as well as 'aminoacyl tRNA biosynthesis', 'glycosyl-phosphatidylinositol GPI anchor biosynthesis', 'RNA degradation' and 'lysine degradation'. In the process, ZNF385D-AS2 also affects signal transfer, material transport within the cell and the progression of various diseases, including pathways for 'acute myeloid leukemia', 'hepatitis' and 'endometrial cancer'. Moreover, simultaneously with the gradual decrease in the expression of this special lncRNA, the expression of tumor-suppressor genes and oncogenes are also altered.

To further explore the biological role of ZNF385D-AS2 in HCC, we conducted a comparative analysis of the data from the TCGA and GEO databases and found approximately 59 genes that may be closely related to this special lncRNA. After functional enrichment of these genes with GO, we found that these genes play an important role in the following biological behaviors, such as molecular function (MF) (growth factor activity, transforming growth factor β receptor binding), biological process (BP) (axon guidance, cell development, regulation of MAPK cascade, positive regulation of cell division, positive regulation of pathway-restricted SMAD protein phosphorylation, cell growth, SMAD protein signal transduction) and cellular component (CC) (extracellular space). The result of the KEGG pathway analysis suggested that these genes can affect signaling pathways including material metabolism within HCC cells, signal transduction, progression of various diseases, and other biological behaviors. After integrating the data in TCGA and GEO, we obtained a total of 96 pairs of co-expressed gene pairs, including 59 genes of different types include mRNAs, miRNAs and lncRNAs. Finally, these data were integrated with gene expression and predicted for possible ceRNA regulatory network and the co-expression network. Finally, we performed whole-genome mapping by GRCh38.95, covering 96 co-expressed gene pairs representing the highest expression difference regions of the cancer genome. This allowed chained links to be directly observed without the need for complex algorithmic inferences reliant on intricate assumptions.

To the best of our knowledge, the present study, for the first time, confirmed that ZNF385D-AS2 greatly affects liver cancer prognosis. The present study, accompanied by other research on liver cancer, elucidated the importance of ZNF385D-AS2. Nevertheless, these findings should be verified in future studies with clinical trials, so as to ensure that ZNF385D-AS2 can be widely applied in the prognostic evaluation of liver cancer.

In conclusion, our study found that low expression of ZNF385D-AS2 was significantly decreased in HCC patients and is associated with several clinical features and a poor prognosis. Thus, ZNF385D-AS2 may be a useful biomarker for the prognosis of patients with liver cancer.

Acknowledgements

Not applicable.

Funding

This study was supported by the Fundamental Research Funds for the Central Universities, JLU, the National Natural Science Foundation of China (Grant No. 31771093), the Project of International Collaboration of Jilin Province (No. 201180414085GH), the Fundamental Research Funds for the Central Universities, JLU, the Program for JLU Science and Technology Innovative Research Team (2017TD-27, 2019TD-36). The funders had no role in study design, data collection and analysis, decision to publish, or preparation of the manuscript.

Availability of data and materials

The Cancer Genome Atlas-Liver Hepatocellular Carcinoma (TCGA-LIHC) and Gene Expression Omnibus (GEO) (GEO-GSE54236).

Authors' contributions

ZZ and SW conceived the presented the research design of the study. YL developed the theory and performed the computations. ZM and FC verified the analytical methods. YL supported ZZ with conducting the experimental research, organized the experimental data into the manuscript and supervised the findings of this work. All authors commented on drafts and approved the final version. All authors participated in the decision to submit for publication. All authors read and approved the manuscript and agree to be accountable for all aspects of the research in ensuring that the accuracy or integrity of any part of the work are appropriately investigated and resolved.

Ethics approval and consent to participate

Not applicable.

Patient consent for publication

Not applicable.

Competing interests

The authors declare that they have no competing interests.

References

1. Hartke J, Johnson M and Ghabril M: The diagnosis and treatment of hepatocellular carcinoma. *Semin Diagn Pathol* 34: 153-159, 2017.

2. Lee Y, Park H, Lee H, Cho JY, Yoon YS, Choi YR, Han HS, Jang ES, Kim JW, Jeong SH, *et al*: The clinicopathological and prognostic significance of the gross classification of hepatocellular carcinoma. *J Pathol Transl Med* 52: 85-92, 2018.
3. Goossens N, Sun X and Hoshida Y: Molecular classification of hepatocellular carcinoma: Potential therapeutic implications. *Hepat Oncol* 2: 371-379, 2015.
4. Liz J and Esteller M: lncRNAs and microRNAs with a role in cancer development. *Biochim Biophys Acta* 1859: 169-176, 2016.
5. Chandra Gupta S and Nandan Tripathi Y: Potential of long non-coding RNAs in cancer patients: From biomarkers to therapeutic targets. *Int J Cancer* 140: 1955-1967, 2017.
6. Zhang Z, Liu F, Yang F and Liu Y: Knockdown of OIP5-AS1 expression inhibits proliferation, metastasis and EMT progress in hepatoblastoma cells through up-regulating miR-186a-5p and down-regulating ZEB1. *Biomed Pharmacother* 101: 14-23, 2018.
7. Zhu X, Liu Y, Yu J, Du J, Guo R, Feng Y, Zhong G, Jiang Y and Lin J: lncRNA HOXA-AS2 represses endothelium inflammation by regulating the activity of NF- κ B signaling. *Atherosclerosis* 281: 38-46, 2019.
8. Samur MK: RTCGAToolbox: A new tool for exporting TCGA firehose data. *PLoS One* 9: e106397, 2014.
9. Villa E, Critelli R, Lei B, Marzocchi G, Camma C, Giannelli G, Pontisso P, Cabibbo G, Enea M, Colopi S, *et al*: Neoangiogenesis-related genes are hallmarks of fast-growing hepatocellular carcinomas and worst survival. Results from a prospective study. *Gut* 65: 861-869, 2016.
10. Zubiete-Franco I, Garcia-Rodriguez JL, Lopitz-Otsoa F, Serrano-Macia M, Simon J, Fernandez-Tussy P, Barbier-Torres L, Fernandez-Ramos D, Gutierrez-de-Juan V, Lopez de Davalillo S, *et al*: SUMOylation regulates LKB1 localization and its oncogenic activity in liver cancer. *EBioMedicine* 40: 406-421, 2019.
11. Jiao Y, Fu Z, Li Y, Meng L and Liu Y: High EIF2B5 mRNA expression and its prognostic significance in liver cancer: A study based on the TCGA and GEO database. *Cancer Manag Res* 10: 6003-6014, 2018.
12. Ginestet C: ggplot2: Elegant graphics for data analysis. *J R Statist Soc A* 174: 245-245, 2011.
13. Lin H and Zelterman D: Modeling survival data: Extending the cox model. *Technometrics* 44: 85-86, 2002.
14. Robin X, Turck N, Hainard A, Tiberti N, Lisacek F, Sanchez JC and Müller M: pROC: An open-source package for R and S+ to analyze and compare ROC curves. *BMC Bioinformatics* 12: 77, 2011.
15. Subramanian A, Tamayo P, Mootha VK, Mukherjee S, Ebert BL, Gillette MA, Paulovich A, Pomeroy SL, Golub TR, Lander ES and Mesirov JP: Gene set enrichment analysis: A knowledge-based approach for interpreting genome-wide expression profiles. *Proc Natl Acad Sci USA* 201: 15545-15550, 2005.
16. Huang da W, Sherman BT and Lempicki RA: Systematic and integrative analysis of large gene lists using DAVID bioinformatics resources. *Nat Protoc* 4: 44-57, 2009.
17. Zhang B and Horvath S: A general framework for weighted gene co-expression network analysis. *Stat Appl Genet Mol Biol* 4: Article17, 2005.
18. Deng Y, He R, Zhang R, Gan B, Zhang Y, Chen G and Hu X: The expression of HOXA13 in lung adenocarcinoma and its clinical significance: A study based on the cancer genome atlas, oncomine and reverse transcription-quantitative polymerase chain reaction. *Oncol Lett* 15: 8556-8572, 2018.
19. Chan EKF, Cameron DL, Petersen DC, Lyons RJ, Baldi BF, Papenfuss AT, Thomas DM and Hayes VM: Optical mapping reveals a higher level of genomic architecture of chained fusions in cancer. *Genome Res* 28: 726-738, 2018.
20. Choi S, Lee S, Kim Y, Hwang H and Park T: HisCoM-GGI: Hierarchical structural component analysis of gene-gene interactions. *J Bioinform Comput Biol* 16: 1840026, 2018.
21. Maciukiewicz M, Marshe VS, Tiwari AK, Fonseka TM, Freeman N, Kennedy JL, Rotzinger S, Foster JA, Kennedy SH and Müller DJ: Genome-wide association studies of placebo and duloxetine response in major depressive disorder. *Pharmacogenomics J* 18: 406-412, 2018.
22. Xu C, Aragam N, Li X, Villla EC, Wang L, Briones D, Petty L, Posada Y, Arana TB, Cruz G, *et al*: BCL9 and C9orf5 are associated with negative symptoms in schizophrenia: Meta-analysis of two genome-wide association studies. *PLoS One* 8: e51674, 2013.
23. Rose JE, Behm FM, Drgon T, Johnson C and Uhl GR: Personalized smoking cessation: Interactions between nicotine dose, dependence and quit-success genotype score. *Mol Med* 16: 247-253, 2010.



This work is licensed under a Creative Commons Attribution-NonCommercial-NoDerivatives 4.0 International (CC BY-NC-ND 4.0) License.